A&A manuscript no.
(will be inserted by hand later)

Your thesaurus codes are:
03.13.7; 08.16.5; 09.03.1; 09.04.01; 09.13.2

ASTRONOMY
AND
ASTROPHYSICS
1.10.1996

The 6.0 and 6.8 μm absorption features in the spectrum of NGC 7538 : IRS9 ⋆

W. A. Schutte[1], A. G. G. M. Tielens[2], D. C. B. Whittet[3], A. Boogert[4], P. Ehrenfreund[1], Th. de Graauw[4], T. Prusti[5], E. F. van Dishoeck[1], P. Wesselius[4]

[1] Leiden Observatory, P. O. Box 9513, 2300 RA Leiden, the Netherlands
[2] NASA Ames Research Center, MS 245-6, Moffett Field, CA 94035, USA
[3] Department of Physics, Applied Physics & Astronomy, Rensselaer Polytechnic Institute, Troy, NY 12180, USA
[4] SRON Laboratory for Space Research, P.O. Box 800, 9700 AV Groningen, the Netherlands
[5] ISO Science Operations Centre, Astrophysics Division, ESA, Villafranca del Castillo,, P.O. Box 50727, 28080 Madrid, Spain

Received <date>, accepted <date>

Abstract. Short Wavelength Spectrometer observations of the 6.0 and 6.8 μm absorption features towards the obscured young stellar object NGC 7538 : IRS9 are presented and compared to the features of a number of species measured in the solid phase. It is found that while solid H_2O provides the bulk of the 6 μm band, additional absorption is required near 5.83 μm and 6.25 μm. It is proposed that formic acid (HCOOH) is a plausible candidate for the blue excess, while the red excess could be related to the C-C stretching mode in aromatic structures. Subsequently, a number of candidates for the 6.8 μm band are reviewed. Unfortunately, none of these appears to satisfy the observational constraints and no plausible identification can at this point be presented.

Key words: ISM: dust, extinction – ISM: molecules – Infrared: ISM: lines and bands – stars: pre-main-sequence – Stars: individual: NGC 7538 : IRS9

1. Introduction

Low resolution airborne spectroscopy of luminous young stellar objects (YSO's) shows two broad absorption features at 6.0 and 6.8 μm (Tielens et al. 1984, Tielens & Allamandola 1987). The 6.0 μm feature has generally been assigned to the bending mode of solid H_2O (Tielens & Allamandola 1987), which is supported by the presence of the H_2O stretching mode at 3 μm. Various assignments have been proposed for the 6.8 μm band, but no candidate has gained general acceptance (e.g., Schutte 1996). Presently, the availability of high resolution, high S/N spectra of ISO's Short Wavelength Spectrometer (SWS) over the full wavelength region warrants a new investigation of these features.

We focus here on one object, the highly embedded massive YSO NGC 7538 : IRS9, which shows some of the strongest solid state absorption features (Tielens et al. 1991). SWS data were obtained in the 5.3 – 8.3 μm region in the full grating mode (AOT06). Being a point source (Willner et al. 1982), the original resolution of the NGC 7538 : IRS9 data was equal to the instrumental resolution in this region (R $\approx$ 1600). To optimize S/N, the resolution was decreased to 600 by a Gaussian smoothing procedure. In view of the considerable width of the 6.0 and 6.8 μm bands ($\sim$ 0.5 μm), this has no effect on the intrinsic shapes. The standard SWS flux calibration, as described by de Graauw et al. (1996) and Schaeidt et al. (1996) was carried out. Treatment of the individual up and down detector scans is described in Boogert et al. 1996.

The spectrum is shown in Fig. 1. It clearly shows the broad 6.0 and 6.8 μm absorption features as well as a sharper dip near 7.7 μm. For comparison the grating spectral response function is also shown. There is no indication of residual structure in the spectrum related to this function. We carefully conclude that the shape of the 6.0 and 6.8 μm absorption bands is robust.

The 7.7 μm band has been identified with solid CH_4 and is discussed in another paper in this volume (Boogert et al. 1996). In the following we discuss the broad bands on the basis of a comparison with the features of various candidates as measured in laboratory simulation experiments. For details on the experimental procedures, see Gerakines et al. (1995).

2. The continuum

The baseline definition over the 5.25 – 8.0 μm region faces some problems. While ice or organic matrices generally show

Send offprint requests to: W. A. SCHUTTE

⋆ ISO is an ESA project with instruments funded by ESA Member States (especially the PI countries: France, Germany, the Netherlands and the United Kingdom) and with the participation of ISAS and NASA.

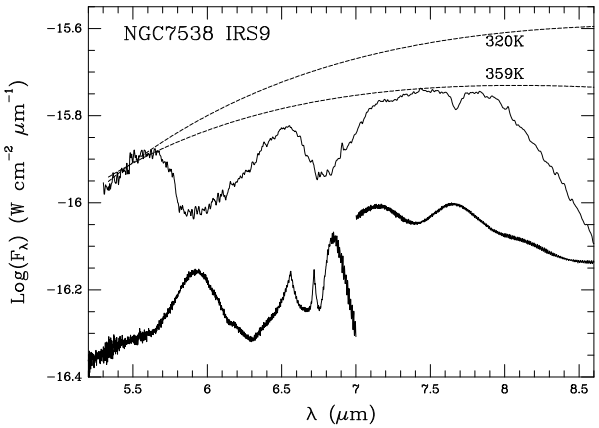

Fig. 1. The upper curve shows the SWS AOT06 observations of the 6.0 and 6.8 μm towards NGC 7538 : IRS9. Two baseline extremes are shown, corresponding to 320 and 359 K black bodies. The grating spectral response functions are shown below the observations.

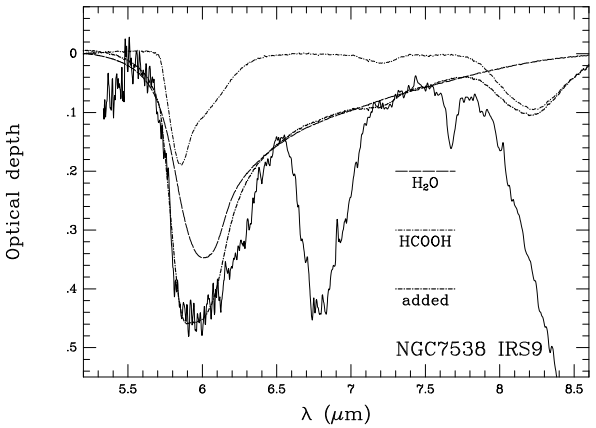

Fig. 2. Optical depth plot obtained from the observations relative to the 359 K blackbody (Fig. 1). The 6.0 μm feature is compared to solid H_2O at 10K, solid HCOOH at 10K, and to the sum of these spectra.

no appreciable absorption blue of 5.60 μm , the region 7.1–8.0 μm does contain absorption bands. In particular, the H_2O bending mode extends out to 7.7 μm (Hudgins et al. 1993), while the 9.7 μm silicate band may extend into the red end of this region as well. In order to assess the resulting uncertainty in the 6.0 and 6.8 μm band shapes we defined baselines under two extreme assumptions (Fig. 1). First we used a 359 K black body. This curve runs through the 5 - 5.6 μm region as well as touches the observed spectrum at 7.50 μm. It thus neglects possible absorption at this position and its slope might therefore be somewhat too shallow. The second extreme is represented by a 320 K black body. This curve follows the steep slope in the 5.25–5.60 μm region, and hence stays considerably above the observed flux level at 7.50 μm. Indeed, a comparison with the overall SWS01 spectrum (Whittet et al. 1996) suggests that this continuum is somewhat too steep. The optical depth plots obtained by subtracting either baseline give very similar results for the 6.8 μm feature. Furthermore no significant variation is observed for the blue wing and the peak position of the 6.0 μm feature. However, a considerable variation is obtained for the red wing of this band. It is considerably deeper for the 320 K baseline, i.e., the 6.0 μm band appears in this case to be more extended towards the red. While keeping the uncertainty in the extension and depth of the red wing in mind, we will use in the remainder the optical depth plot obtained by subtracting the 359 K blackbody for comparison with the laboratory data (Fig. 2).

3. Comparison with laboratory data

3.1. The 6.0 μm feature

As discussed in Section 1, the 6.0 μm feature has previously been ascribed to the bending mode of solid H_2O. Fig. 2 compares H_2O ice deposited at 10 K with NGC 7538 : IRS9. It can be seen that, while the position of the interstellar feature is well matched by H_2O, the observed band is considerably broader, i.e., shows extra red and blue absorption. This discrepancy cannot be remedied by warm-up of the ice (e.g., Hudgins et al. 1993). The baseline uncertainty tends to increase the discrepancy (Section 2). Furthermore, calculations show that particle shape effects are negligible for this feature. We conclude that additional components must contribute to the 6.0 μm band.

The blue excess is centered near 5.83 μm and has FWHM $\approx$ 0.17 μm. This position is characteristic of the C=O stretching mode in organic molecules. For amides (R–$CONH_2$) this mode is too blue (5.93 μm). Furthermore, aldehydes (R-HCO, e.g., H_2CO) give a too narrow band (FWHM 0.07 – 0.10 μm). However, organic acids (R–COOH) may provide a good fit to the blue excess. This is illustrated in Fig. 2 which shows a fit of the 6.0 μm band with the combined features of H_2O and formic acid (HCOOH) at 10 K. Using a band strength of 6.7 x 10^{-17} cm for the C=O stretching mode (Maréchal 1987), the abundance of HCOOH obtained from Fig. 2 equals 3 % ($\pm$ 1 %) of H_2O. While higher organic acids should also be able to match the blue excess, it seems likely that the simplest acid, HCOOH, is most readily produced. The column density of the H_2O component of the 6.0 μm band, as shown in Fig. 2, equals 8.0 10^{18} cm^{-2}, in close agreement with the value obtained from the 3 μm feature (Allamandola et al. 1992). With a hydrogen column density N(H) = 1.6 10^{23} cm^{-2} (Tielens et al. 1991), the H_2O abundance than equals 5 10^{-5}. Besides the 5.85 μm band, HCOOH has strong features at 3.06 and 8.2 μm, which however blend with the H_2O and silicate features. In addition, it shows two weak bands at peak strength of $\sim$ 10 % of the 5.85 μm feature at 3.87 and 7.23 μm. A hint of the latter feature may perhaps be present in the observations (Fig. 2).

Due to its relatively large peak intensity (close to that of CO), particle shape effects could be of some importance if HCOOH would reside in a rather pure form in interstellar ice.

However, it appears likely that the HCOOH would rather be severely diluted, and in this case such effects should be negligible (Tielens et al. 1991). Of course, in that case the intrinsic profile of the C=O stretching mode may change somewhat. A full investigation of all these aspects of the HCOOH assignment of the blue excess of the 6.0 μm band, as well as a discussion of possible formation mechanisms, is deferred to a later paper.

The red excess is centered at $\sim$ 6.25 μm and has a width of $\sim$ 0.2 μm. The position and width suggest that C-C stretching modes of aromatic structures in carbonaceous solids might contribute. This would make this feature the absorption counterpart of the well-known 6.2 μm PAH emission feature. The equivalent width of the red excess is $\sim$ 8 cm^{-1}, implying that about 20 % of C along the line-of-sight would be included in aromatic structures (using N(C)/N(H) = 4 10^{-4}, N(H) = 1.6 10^{23} cm^{-2} towards NGC 7538 : IRS9 (Tielens et al. 1991), and σ_{int} = 2 10^{-19} cm/C atom (Schutte et al. 1993)). Such an abundance for carbonaceous solids appears reasonably consistent with models of the refractory component of interstellar grains (Mathis et al. 1983, Greenberg & Chlewicki 1983). It must be noted that the additional very broad aromatic C-C stretch near 7.7 μm would be very hard to distinguish due to the presence of the 6.8 μm band and the onset of the silicate absorption. At a reasonable degree of hydrogenation for such carbonaceous solids (H/C $\approx$ 0.2) the strength of the 3.3 and 11.3 μm C-H modes would be similar to the 6.2 μm band (Papoular et al. 1991, Guillois et al. 1996) and could perhaps be observed with highly sensitive spectroscopy. Indeed, the detection of a feature near 3.25 μm which possibly corresponds with the aromatic C-H stretching mode was recently reported for a number of YSO's (Brooke et al. 1996, Sellgren et al. 1995). It must be noted that the strength of the red excess depends quite sensitively on the baseline definition; with the 320 K baseline (section 2), its equivalent width increases by approximately a factor of 2.

In summary, we propose that the 6.0 μm absorption feature is contributed by (at least) 3 different components, i.e., H_2O, an organic acid such as HCOOH, and a component responsible for the red excess absorption, possibly a refractory carbonaceous solid. In this view ISO will likely reveal source to source variations of the shape of the 6.0 μm feature.

3.2. The 6.8 μm feature

An obvious candidate for the 6.8 μm feature is the C-H deformation mode of organic species. While for R-CH_2-R and R-CH_3 groups the mode is too narrow, for alcohols (R-HCOH-R) the feature broadens considerably due to the interaction between the CH and OH deformation modes. In particular CH_3OH provided a fairly good match to earlier, low resolution Kuiper Airborne spectra (Tielens & Allamandola 1987, Tielens et al. 1984).

Fig. 3 shows a comparison of the 6.8 μm feature with a composite spectrum produced by adding the composite H_2O/HCOOH spectrum (Fig. 2) to a spectrum of pure solid CH_3OH, deposited at 10 K (Hudgins et al. 1993). It can be seen that the methanol feature falls somewhat red of the interstellar band. The methanol feature does not shift in ices dominated by

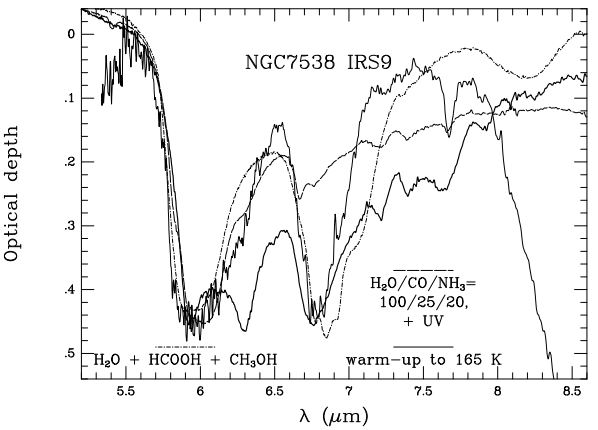

Fig. 3. A comparison of the 6.8 μm feature with the sum of the spectrum of 10 K solid CH_3OH (from Hudgins et al. 1993) and the H_2O + HCOOH combination spectrum of Fig. 2. Additionally, a comparison of the 6.8 μm feature with the NH_4^+ feature obtained by UV photolysis of a $H_2O/CO/NH_3$ = 100/25/20 at 10 K, and after warm-up to 165 K.

H_2O, giving an equally imperfect match (Hudgins et al. 1993). The discrepancy can neither be remedied through warm-up, or by diluting with apolar material, e.g., no shift is seen for $H_2O/CH_3OH/CO_2$ = 100/40/60. Perhaps the imperfect match of the red wing reflects to some extent the uncertainty in the choice of the continuum. Indeed, the 320 K baseline (Section 2) produces a 6.8 μm band which corresponds slightly better with the methanol feature, and an even steeper baseline would produce further improvement. However, besides the imperfect match, an assignment to methanol faces serious problems with regard to the absence of additional features. The strength of the CH bending mode would require C-H and C-OH stretching modes near 3.54 μm and 9.7 μm of τ = 0.5 and 1, respectively (d'Hendecourt & Allamandola 1986). Especially the 9.7 μm feature, which is much narrower than the silicate band, should be highly conspicuous but is clearly not observed anywhere near the required strength in the SWS01 scan of NGC 7538 : IRS9 (Whittet et al. 1996). While Allamandola et al. (1992) detected the methanol C-H stretch band, the corresponding abundance is $\sim$ 4 times less than necessary to account for the 6.8 μm band. Thus while CH_3OH contributes to the 6.8 μm band at the 25 % level, most of it has to be carried by another species.

An assignment to higher alcohols faces similar problems. Higher alcohols with R-CH_3 groups, e.g., ethanol, show a strong, sharp, deformation mode at 7.25 μm, and can be excluded. Thus, only species which have an -OH attached to every C atom appear possible. In a mixture of $H_2O/HOCH_2CH_2OH \approx$ 100/20, deposited at 10K, the feature falls at $\sim$ 6.90 μm, producing a slightly worse fit than methanol. Moreover, like CH_3OH, higher alcohols show strong C-H and C-OH stretching modes near 3.4 and 9.5 μm, which should be highly conspicuous but are not observed. We conclude that an assignment of the bulk of the interstellar 6.8 μm feature to the CH bending modes in alcohols can generally be excluded.

Alternatively, it has been proposed that the 6.8 μm feature may originate in interstellar carbonates (e.g.; $MgCO_3$; Sandford & Walker 1985). However, carbonates show an additional feature near 11.6 μm, at approximately half the peak strength, but with a considerably smaller width (FWHM $\approx$ 0.15 μm; Sandford & Walker 1985). This band should be superimposed on the silicate 10 μm band, but is not observed in the SWS01 scan of NGC 7538 : IRS9 (Whittet et al. 1996). We conclude that an assignment to carbonates is unlikely.

Finally, an assignment to the NH_4^+ ion has been considered (Grim et al. 1989a). This species was created in the laboratory by irradiation of ices containing H_2O, CO and NH_3. The reaction path involves the photochemical formation of acids (e.g., HNCO, HCOOH) followed by proton exchange with the base NH_3 (Grim et al. 1989b). Fig. 3 shows a comparison with an ice mixture of original composition $H_2O/CO/NH_3$ = 100/25/20 following photolysis at 10 K, and after warm-up to 165 K. It can be seen that the NH_4^+ band is much too weak and furthermore falls somewhat longward of the 6.8 μm feature in the 10 K ice. A rather good match both in position and strength relative to the 6.0 μm H_2O band is obtained after partial H_2O sublimation at 165 K. The shift appears to be induced by the H_2O sublimation since it occurs exclusively over the 160 – 180 K interval where the sublimation takes place. However, besides the NH_4^+ band, a number of other features are apparent in the lab spectra which are not present in the observations (cf., Grim et al. 1989b).

Perhaps the most important objection to the NH_4^+ identification is the absence of absorptions due to suitable counterions. In the photolyzed residues, the 6.33 and 7.41 μm bands are attributed to a counterion, $HCOO^-$. This is a very general problem. All ions have strong features, e.g., NO^-, NO_2^-, and NO_3^- absorb strongly in the 5.5 - 8.5 μm range (Grim et al. 1989b). While an assignment of the XCN band observed near 4.62 μm (Lacy et al. 1984, Whittet et al. 1996) with OCN^- has earlier been proposed (Grim & Greenberg 1987), the strength of this feature shows that OCN^- can at most account for $\sim$ 15 % of the necessary counter–charge (Schutte & Greenberg 1996). We therefore conclude at this point that an assignment to NH_4^+ appears unlikely due to the absence of identifiable counterions towards NGC 7538 : IRS9.

In summary, the availability of full ISO spectra allows us to scrutinize a number of proposed assignments for the 6.8 μm band. It is found that no satisfactory candidates are presently available. The observational constraints are nevertheless quite stringent. First, the carrier has no other strong features, since no additional unidentified bands of comparable intensity are observed (Whittet et al. 1996). Second, the feature appears to correlate with the 6.0 μm band rather than with the silicate feature, suggesting an origin in the icy grain mantles (Tielens & Allamandola 1987). If the feature originates in ice, the carrier must be an abundant constituent. For a typical infrared band strength of 1 10^{-17} cm, its abundance would be 30 % of H_2O. Clarifying the nature of the 6.8 μm absorption feature remains one of the major challenges in the study of interstellar ices.

Acknowledgements. This work was partially funded by NASA grant NGR 33-018-148 and by a PIONIER grant from the Netherlands Organization for Scientific Research (NWO). Support by ASTRON and SRON is acknowledged as well. WS mentions inspiring discussions with J. Mayo Greenberg.

References

Allamandola L.J., Sandford S.A., Tielens A.G.G.M., Herbst T.M., 1992, ApJ 399, 134
Boogert A.C.A., Schutte W.A., Tielens A.G.G.M., et al., 1996, this volume
Brooke T.Y., Sellgren K., Smith R.G., 1996, ApJ 459, 209
de Graauw Th., Whittet D. C. B., Gerakines P. A., et al., 1996, this volume
d'Hendecourt L.B., Allamandola L.J., 1986, A&AS 64, 453
Gerakines P.A., Schutte W.A., Greenberg J.M., van Dishoeck E.F., 1995, A&A 296, 810
Guillois O., Nenner I., Papoular R., Reynaud C., 1996, ApJ 464, 810
Greenberg J.M., Chlewicki G., 1983, ApJ 272, 563
Grim R.J.A., Greenberg J.M., 1987, ApJ 321, L91
Grim R.J.A., Greenberg J.M., Schutte W.A., Schmitt B., 1989a, ApJ 341, L87
Grim R.J.A., Greenberg J.M., de Groot M.S., Baas F., Schutte W.A., Schmitt B., 1989b, A&AS 78, 161
Lacy J.H., Baas F., Allamandola L.J., et al., 1984, ApJ 276, 543
Hudgins D.M., Sandford S.A., Allamandola L.J., Tielens A.G.G.M., 1993, ApJS 86, 713
Maréchal Y., 1987, J. Chem. Phys. 87, 6344
Mathis J.S., Mezger P.G., Panagia N., 1983, A&A 128, 212
Papoular R., Reynaud C., Nenner I., 1991, A&A 247, 215
Sandford S.A., Walker R.M., 1985, ApJ 291, 838
Schaeidt et al., 1996, this volume
Schutte W.A., Tielens A.G.G.M., Allamandola L.J., 1993, ApJ 415, 397
Schutte W.A., 1996, in: The cosmic dust connection, Greenberg, J. M. (ed.), in press
Schutte W.A., Greenberg J.M., 1996, submitted to A&A
Sellgren K., Brooke T.Y., Smith R.G., Geballe T.R., 1995, ApJ 449, L69
Tielens A.G.G.M., Allamandola, L.J., Bregman J., Goebel J., d'Hendecourt L.B., Witteborn F.C., 1984, ApJ 287, 697
Tielens A.G.G.M., Allamandola L.J., 1987, in: Physical processes in interstellar clouds, Morfill, G.E., Scholer, M. (eds.). Reidel, Dordrecht, p. 333
Tielens A.G.G.M., Tokunaga A.T., Geballe T.R., Baas F., 1991, ApJ 381, 181
Whittet D.C.B., Schutte W.A., Tielens A.G.G.M., et al., 1996, this volume
Willner S.P., Gillett F.C., Herter T.L., et al., 1982, ApJ 253, 174.

This article was processed by the author using Springer-Verlag TEX A&A macro package 1992.